

Protective effect of overexpression of PrxII on H₂O₂-induced cardiomyocyte injury

T. GAO, X.-X. CHE, R. WANG, C.-S. XIAO, Y.-P. JIA

Department of Cardiology, First Hospital of Shanxi Medical University, Taiyuan, China

Abstract. – OBJECTIVE: Oxidative stress is one of the main factors leading to myocardial cell damage, and the redox imbalance promotes apoptosis. Therefore, the purpose of this study was to explore the protective effect of PrxII on H₂O₂-induced H9c2 cell injury.

MATERIALS AND METHODS: The overexpressed PrxII cell model was constructed by virus. The H9c2 cells were treated with H₂O₂, and the supernatant and cells were collected. Then, the chymotrypsin-like activity, caspase-like activity, and trypsin-like activity were detected by the kit, and the expressions of P21, P27, and P53 were detected by the ELISA method. Finally, the expressions of antioxidant factors, apoptosis-related factors, and AMPK/Sirt1 signaling pathway were detected by Western blot and Real-time polymerase chain reaction (PCR).

RESULTS: Overexpression of PrxII inhibited the decrease of enzyme activity induced by H₂O₂, promoted the expressions of anti-oxidation factors GPX1, GPX2, and GSX, and inhibited the expressions of apoptosis-related factors P21, P27, and P53, and activated AMPK/Sirt1 pathway.

CONCLUSIONS: Overexpression of PrxII can activate the AMPK/Sirt1 pathway, thereby inhibiting H₂O₂-induced oxidative stress and slowing apoptosis.

Key Words:

PrxII, H9c2, Oxidative stress, Apoptosis, AMPK/Sirt1 pathway.

Abbreviations

Ischemia-reperfusion injury (I/R injury); reactive oxygen species (ROS); superoxide dismutase (SOD); 5' AMP-activated protein Kinase/Sirt1 (AMPK/Sirt1); acetyl-CoA carboxylase (ACC); Dulbecco's Modified Eagle's Medium (DMEM); fetal bovine serum (FBS); phosphate-buffered saline (PBS); sodium dodecyl sulphate (SDS); Polymerase Chain Reaction (PCR); complementary deoxyribose nucleic acid (cDNA); glyceraldehyde 3-phosphate dehydrogenase (GAPDH); 4',6'-diamidino-2-phenylindole (DAPI); lactate dehydrogenase

(LDH); malondialdehyde (MDA); Enzyme-Linked Immunosorbent Assay (ELISA); optical density (OD); Statistical Product and Service Solutions (SPSS); analysis of variance (ANOVA).

Introduction

Cardiovascular diseases have attracted much attention due to their high morbidity and mortality. Among them, ischemia-reperfusion injury (I/R injury), myocardial infarction, and cardiac hypertrophy are common clinical myocardial injury diseases, and also hot fields of cardiovascular research¹. The pathogenic factors of I/R injury are mainly the accumulation of reactive oxygen species (ROS), which induces myocardial cell necrosis, apoptosis, DNA damage, mitochondrial dysfunction, and myocardial systolic dysfunction, etc².

In myocardial ischemia, the activity of antioxidant enzymes is destroyed, the amount of ROS is greatly increased, and accumulation in cells, nucleic acids, proteins, etc. will undergo oxidation reaction, resulting in destruction of cell structure, a large number of proteins folding errors, tissue dysfunction, and a series of stress responses². There are two main antioxidant systems responsible for scavenging excessive ROS: (1) antioxidant enzyme system: superoxide dismutase (SOD) and catalase which can remove excess ROS from the body, (2) Sulfhydryl reduction buffer system: sulfhydryl-based antioxidant-reducing glutathione and oxidized glutathione maintain homeostasis in cells³. Antioxidant protein PrxII belongs to peroxidase super family consisting of 6 members, of which PrxII has been widely concerned due to the superior clearance rate shown in the clearance of ROS^{4,5}. In I/R animals, the protein expression level of PrxII was significantly downregulated, suggesting that PrxII is involved in the development of myocardial injury. There-

fore, the main purpose of this study was to discuss the overexpression of PrxII by adenovirus to protect cardiomyocytes from oxidative stress-induced oxidative stress and apoptosis.

By reviewing the literature, it was found that the AMPK/Sirt1 (5' AMP-activated protein Kinase/Sirt1) signaling pathway plays an important role in cardiomyocytes against oxidative stress and anti-apoptosis⁶. AMPK plays an important role in the energy metabolism of cells and is activated in two ways. One is the allosteric activation of AMPK with the elevation of AMP/ATP. The main role of AMPK activated by this method is to reduce cells, with energy consumed and stored. Another way is that upstream kinase AMPKK phosphorylation activates AMPK, which in turn includes LKB1 and CaMKK⁷. In cardiomyocytes, activated AMPK can lead to phosphorylation of its downstream substrates, such as acetyl-CoA carboxylase (ACC) affecting gene expression, promoting ATP-promoting pathways (such as glycolysis, glucose uptake, mitochondrial proliferation, and increased enzyme activity), while inhibiting ATP-consumption biological processes (such as inhibition of protein synthesis, fat synthesis, etc.). It can be seen that AMPK plays an important role in maintaining cell energy supply and inducing adaptive response, thereby maintaining cell homeostasis⁸.

Materials and Methods

Cell Culture

The H9c2 cells (Cell Culture Center, Shanghai, China) were cultured in a Dulbecco's Modified Eagle's Medium (DMEM, Life Technology, Gaithersburg, MD, USA) containing 100 U/mL penicillin, 100 µg/mL streptomycin, and 10% fetal bovine serum (FBS, Life Technology, Gaithersburg, MD, USA) in a 5% CO₂ cell culture incubator at 37°C. After the cells covered the bottom of the bottle, they were digested with 0.25% trypsin digest, and the cells in the logarithmic growth phase were subjected to the following experiments.

Transfection

After H9c2 cell counting, the platelet density of myocardial cells in each well of 6-well plate reached 70-80%. After 6 days of culture, the amount of each virus at 200 MOI was calculated, and an appropriate amount of virus solution (Shanghai Jikai Gene Chemical Technology, Shanghai, China) was added. Then, the medium was replaced to continue the culture of the cells.

After 48 h, the fluorescence state of the cells was observed by a fluorescence microscope, and the corresponding expression levels of the cell protein and total RNA were detected to ensure the success of the virus infection.

Experimental Grouping

Stably transfected H9c2 cells were adjusted to a cell density of 1×10^4 cells/mL and seeded in 96-well plates (100 µL/well), and the marginal wells were filled with phosphate-buffered saline (PBS). After 24 h of cell culture, the wells were treated with H₂O₂ in sequence. The control group was added with blank culture medium. The above cells were divided into control group, H₂O₂ group, Lenti-PrxII group, Lenti-NC group, and then the cell culture plates in the above groups were further transferred into the incubator for subsequent experiments.

Proteasome Activity Assay

The HEPES solution (KeyGEN, Nanjing, China) was configured as a tissue sample homogenate, and the myocardial protein was extracted and quantified. The fluorescent substrates Z-LLE-AMC, Ac-RLR-AMC, and Suc-LLUY AMC (KeyGEN, Nanjing, China) were diluted with HEPES solution to a concentration of 45 mM, 40 mM, and 18 mM. In a 96-well plate, 200 µL of substrate solution and 10 µg of protein were added, placed in an incubator in the dark, and allowed to stand at 37°C for 1 h. In the microplate reader, the excitation wavelength of 380 nm and the emission wavelength of 460 nm were set to detect the fluorescence value in the well.

Western Blot

Each group of cells was collected, and 1 mL of cell lysate was added, ultrasonically pulverized and centrifuged. Then, the supernatant was taken. 20 µg of sample protein/well was loaded separately, protein was separated by sodium dodecyl sulphate (SDS) polyacrylamide gel electrophoresis, wet for 1 h (4°C, 100 V), 5% skim milk powder was blocked for 2 h, and then, flattened with primary antibody (GPX1, Abcam, Cambridge, MA, USA, 1:1000, GPX2, Abcam, Cambridge, MA, USA, 1:1000, GSR, Abcam, Cambridge, MA, USA, 1:1000, PrxII, Abcam, Cambridge, MA, USA, 1:2000, Sirt1, Abcam, Cambridge, MA, USA, 1:2000, Bmi-1, Abcam, Cambridge, MA, USA, 1:2000, P21, Abcam, Cambridge, MA, USA, 1:2000, AMPK, Abcam, Cambridge, MA, USA, 1:1000, p-AMPK, Abcam, Cambridge, MA, USA, 1:500, PGC-α, Abcam, Cambridge,

MA, USA, 1:1000, GAPDH, Abcam, Cambridge, MA, USA, 1:5000) at 4°C. After shaking overnight, the horseradish peroxidase (HRP)-labeled secondary antibody was incubated for 2 h in the dark. The color was developed with a color developing solution, and the band was obtained by chemiluminescence (Thermo Fisher Scientific, Waltham, MA, USA). After scanning the film, the gray scale analysis of the target band was performed using IPP 6.0 software (Media Cybernetics, Silver Springs, MD, USA) to calculate the relative expression of the above protein.

Total RNA Extraction and Real Time-Polymerase Chain Reaction (PCR)

The total RNA of each group of cells was extracted by total RNA extraction kit (Thermo Fisher Scientific, Waltham, MA, USA), reverse transcription was performed to obtain complementary deoxyribose nucleic acid (cDNA), and 2 µL was taken for PCR amplification. The assay factors and internal reference amplification conditions: pre-denaturation at 94°C for 2 min for 1 cycle, denaturation at 94°C for 30 s, annealing at 55°C for 30 s and extension at 72°C for 2 min for 35 cycles, and total extension at 72°C for 6 min. Analysis of results: using glyceraldehyde 3-phosphate dehydrogenase (GAPDH; Thermo Fisher Scientific, Waltham, MA, USA) as an internal reference, the corresponding $-\Delta\Delta C_t$ values in each group of cells were calculated, and the quantitative analysis was performed based on the quantitative amount of the target gene ($2^{-\Delta\Delta C_t}$). All the primers are listed in Table I.

Immunofluorescence

H9c2 cells in each group were fixed by adding 4% paraformaldehyde into the culture plate for

15 min and washed with PBS for 3 times with 3 min/time. Then, 10% goat serum was added and sealed for 1 h. The diluted primary antibody (PGC-1 α , 1:500, Abcam, Cambridge, MA, USA) was used for incubation overnight at 4°C. The next day, fluorescence secondary antibody was added for incubation in dark for 1h. Then, 4',6-diamidino-2-phenylindole (DAPI; Thermo Fisher Scientific, Waltham, MA, USA) was added for incubation for 15 min in the dark. After that, the tablets were sealed with the sealing tablet, and then the images were observed and collected under the fluorescence microscope.

Detection of Biochemical Indicators

The cell supernatants of each group were collected, the working solution was configured using a commercial kit, and then the supernatant of the cells was added to determine the levels of superoxide dismutase (SOD), lactate dehydrogenase (LDH), and malondialdehyde (MDA) in each group (Jiancheng, Nanjing, China).

Active Oxygen Detection

Each group of H9c2 cells was collected, and the Reactive Oxygen Species (ROS) levels in each group were measured using an active oxygen detection kit (Jiancheng, Nanjing, China) according to the manufacturer's instructions.

Enzyme-Linked Immunosorbent Assay (ELISA)

The supernatants of each group of cells were collected and centrifuged. The control wells and the sample wells were set according to the kit instructions (Jianglai, Shanghai, China), the corresponding standards were added to the control wells, and all the wells were added with the corresponding

Table I. Real time PCR primers

Gene name	Forward (5'>3')	Reverse (5'>3')
Sirt1	CCAGATCCTCAAGCCATG	TTGGATTCCTGCAACCTG
GSR	GACACCTCTTCCTTCGACTACC	CCCAGCTTGTGACTCTCCAC
GPX1	ATCATATGTGTGCTGCTCGGCTAGC	TACTCGAGGGCACAGCTGGGCCCTTGAG
GPX2	GCCTCAAGTATGTCCGACCTG	GGAGAACGGGTATCATAAGGG
Bmi-1	ATCCCCACTTAATGTGTGTCTCT	CTTGCTGGTCTCCAAGTAACG
TXN	GTGAAGCAGATCGAGAGCAAG	CGTGGCTGAGAAGTCAACTACTA
AMPK	AAAGAACCCTAGCCTGAAGAGG	ACCTTCCGAGATGAATGCTTTT
PGC-1 α	TATGGAGTGACATAGAGTGTGCT	CCACTTCAATCCACCCAGAAAG
P53	CTCTCCCCGCAAAGAAAAA	CGGAACATCTCGAAGCGTTTA
P21	CCTGGTGATGTCCGACCTG	CCATGAGCGCATCGCAATC
GAPDH	ACAACCTTGGTATCGTGGAAGG	GCCATCACGCCACAGTTTC

RT-PCR, quantitative reverse-transcription polymerase chain reaction.

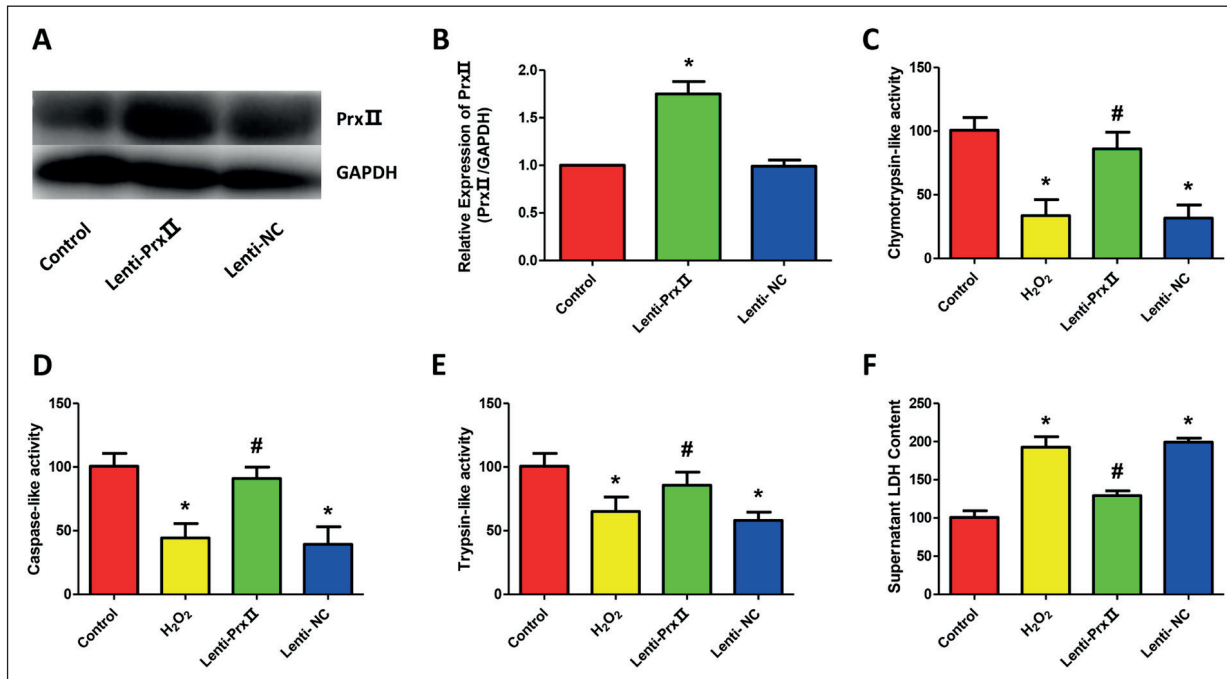


Figure 1. Overexpression of PrxII inhibits H₂O₂-induced H9c2 cell injury. **A**, Western blot verification of transfection. **B**, Real-time PCR verifies transfection. **C**, Chymotrypsin-like activity detection. **D**, Caspase-like activity test. **E**, Trypsin-like activity detection. **F**, LDH content detection. (“*” indicates statistical difference from the control group $p < 0.05$, “#” indicates statistical difference from the contrast group $p < 0.05$).

detection antibodies and incubated at 37°C for 1 h. After discarding the liquid, the working solution was added to each well for incubation for 15 min in the dark. After termination of the stop solution, the optical density (OD) value of each well was measured at a wavelength of 450 nm.

Statistical Analysis

Statistical analysis was performed using Statistical Product and Service Solutions (SPSS) 22.0 (IBM, Armonk, NY, USA). The experimental data were expressed as mean ± standard deviation. Comparison between multiple groups was done using One-way analysis of variance (ANOVA) test followed by Pos-Hoc Test (Least Significant Difference). $p < 0.05$ suggested that the difference was statistically significant.

Results

Overexpression of PrxII Inhibits H₂O₂-Induced H9c2 Cell Injury

First, Western blot and Real-time PCR were used to verify that H9c2 cells were over-expressed with PrxII (Figure 1A and 1B). Second, it was found that overexpression of PrxII re-

duced H₂O₂-induced chymotrypsin-like activity, caspase activity, trypsin-like activity inhibition, and significantly reduced H₂O₂-induced LDH content (Figure 1C-1F). There was no significant difference between NC group and H₂O₂ group.

Overexpression of PrxII Inhibits H₂O₂-Induced H9c2 Oxidative Stress

The expressions of GPX1, GPX2, and GSR were detected by Western blot. It was found that overexpression of PrxII inhibited the expressions of GPX1, GPX2, and GSR induced by H₂O₂ treatment, while there was no significant difference between NC group and H₂O₂ group (Figure 2A and 2B). Similar results were obtained for mRNA level verification. Also, overexpression of PrxII inhibited H₂O₂-induced increase in TXN expression (Figure 2C-2F). The results of the kit showed that the SOD content was decreased significantly after H₂O₂ treatment, and MDA was increased significantly, while overexpression of PrxII could effectively alleviate this phenomenon (Figure 2G-2H). Flow cytometry results also confirmed that overexpression of PrxII significantly inhibited H₂O₂-induced ROS elevation, while NC group ROS levels were not significantly different from H₂O₂ (Figure 2I).

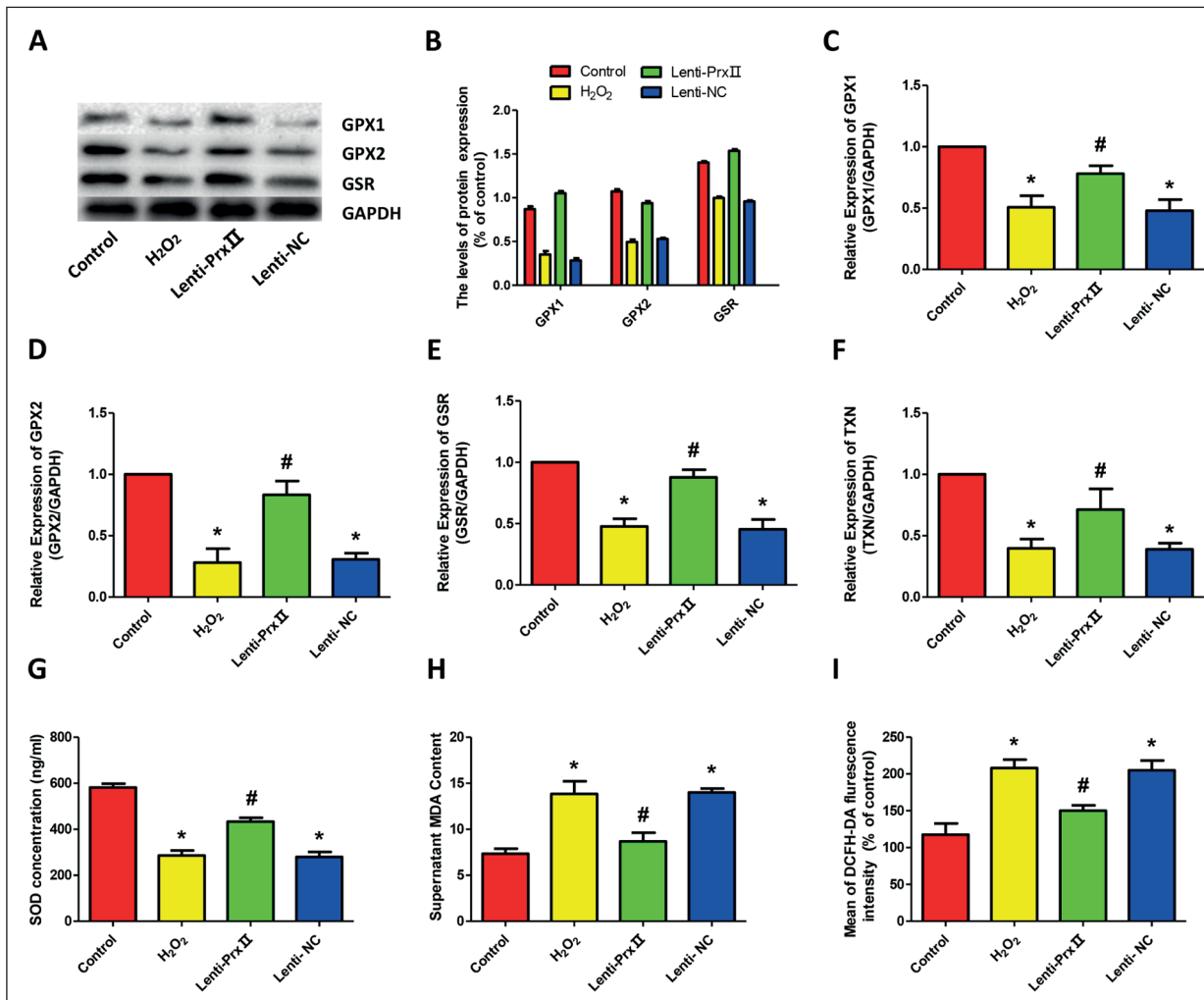


Figure 2. Overexpression of PrxII inhibits H₂O₂-induced H9c2 oxidative stress. **A**, Western blot is used to detect GPX1, GPX2, and GSR expressions. **B**, Protein expression analysis. **C**, GPX1 mRNA expression. **D**, GPX2 mRNA expression. **E**, GSR mRNA expression. **F**, TXN mRNA expression. **G**, SOD content detection. **H**, MDA content detection. **I**, Flow cytometry is used to detect ROS levels. (“*” indicates statistical difference from the control group $p < 0.05$, “#” indicates statistical difference from the contrast group $p < 0.05$).

Overexpression of PrxII Inhibits H₂O₂-Induced Apoptosis in H9c2 Cells

The literature found that oxidative stress damage is closely related to apoptosis. Therefore, the expressions of anti-apoptotic factors Sirt1, Bmi-1, and P21 were first detected. After H₂O₂ treatment of H9c2 cells, the cells expressing Sirt1 and Bmi-1 were significantly decreased, and P21 was significantly increased. However, overexpression of PrxII could significantly promote the expression of Sirt1 and Bmi-1 and inhibit the expression of P21 (Figure 3A and 3B). At the same time, Real-time PCR also obtained similar results that the expressions of P21 and P27 were significantly decreased in overexpressed PrxII group (Figure

3C-3F). Secondly, it was found by ELISA that overexpression of PrxII inhibited H₂O₂-induced P21, P27, and P53 elevation (Figure 3G-3I).

Overexpression of PrxII Activates the AMPK Pathway

The AMPK pathway regulates cellular oxidative stress and apoptosis. Therefore, the expressions of AMPK, p-AMPK, and the downstream factor PGC-1 α were examined by Western blot, and the ratio of p-AMPK/AMPK indicates the activation of AMPK *in vivo*. The results showed that the levels of p-AMPK and p-AMPK/AMPK were significantly lower in the H₂O₂ group than in the control group. Compared with the H₂O₂

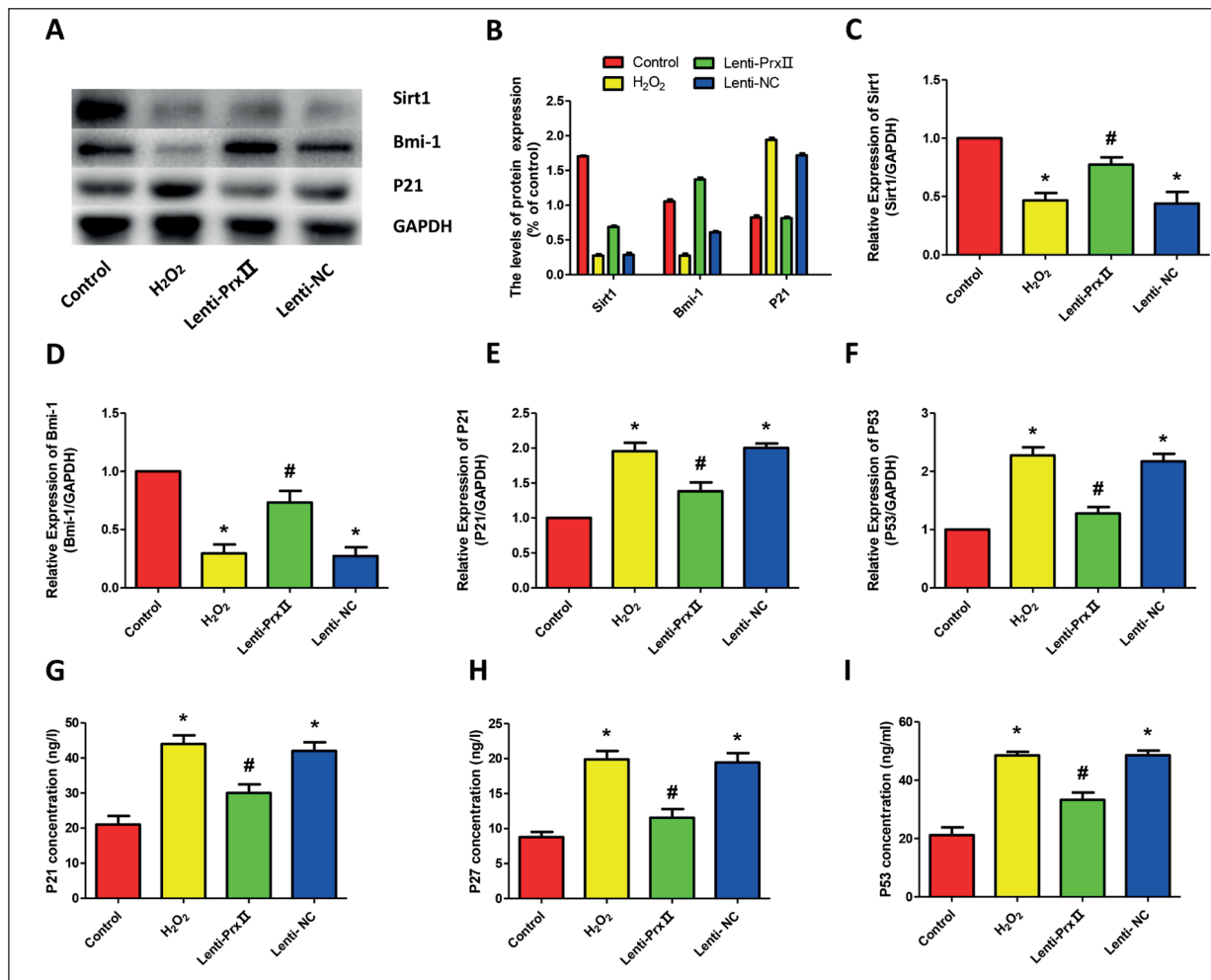


Figure 3. Overexpression of PrxII inhibits H₂O₂-induced apoptosis in H9c2 cells. **A**, Western blot is used to detect the expressions of Sirt1, Bmi-1, and P21. **B**, Protein expression analysis. **C**, Sirt1 mRNA expression. **D**, Bmi-1 mRNA expression. **E**, P21 mRNA expression. **F**, P53 mRNA expression. **G**, Elisa detects the P21 content. **H**, ELISA detects the P27 content. **I**, ELISA detects P53 content. (“*” indicates statistical difference from the control group $p < 0.05$, “#” indicates statistical difference from the contrast group $p < 0.05$).

group, overexpression of the PrxII significantly increased p-AMPK expression and p-AMPK/AMPK levels, with no significant differences between the NC and H₂O₂ groups. Besides, after H₂O₂ treatment, the expression of PGC-1 α was significantly increased, while overexpression of PrxII significantly inhibited the expression of PGC-1 α (Figure 4A). The mRNA results were similar to the former (Figure 4B, 4C). At the same time, immunofluorescence results indicated that the expression of PGC-1 α was significantly increased in H₂O₂ group, while overexpression of PrxII could effectively decrease the expression of PGC-1 α . There was no significant difference between NC group and H₂O₂ group (Figure 4D).

Discussion

The pathogenesis of cardiovascular diseases is complex, and one of the important mechanisms of oxidative stress damage interacts with other pathophysiological processes to promote the progression of cardiovascular disease⁹. Under physiological conditions, the oxidative system and the antioxidant system in the cardiomyocytes are in equilibrium. When factors such as ischemia, hypoxia, and reperfusion are received, the degree of oxide production is greater than the clearance rate, resulting in imbalance of the oxidation system and the antioxidant system in the body, as well as oxidative stress damage¹⁰.

MDA and SOD are hallmarks for assessing the extent of oxidative stress¹¹. The intracellular oxygen free radical activity is very high, and it can rapidly react with substances such as unsaturated fatty acids in the cells to produce MDA. The level of MDA can indirectly reflect the degree of oxidative stress in the body. In contrast, SOD is an intracellular antioxidant enzyme that can scavenge ROS, inhibit oxidative stress damage, and reflect the body's antioxidant levels¹². The results of this study indicated that MDA content was significantly increased in the H₂O₂ group, while overexpression of PrxII inhibited the increase of MDA content and promoted the increase of SOD content, thereby removing excess ROS.

AMPK affects cell energy metabolism and plays a key role in cardiomyopathy. p-AMPK is phosphorylated AMPK, reflecting AMPK activity, and p-AMPK/AMPK ratio indicates activation of AMPK *in vivo*¹³. Researches have shown that intracellular AMPK deficiency can further aggravate cardiac dysfunction in diabetic cardiomyopathy rats, showing that AMPK plays an important role in the regulation of myocardial energy metabolism¹⁴. The results showed that compared with the control group, the levels of p-AMPK

and p-AMPK/AMPK in the H₂O₂ group were significantly decreased, indicating that oxidative stress has a significant effect on energy metabolism in myocardial tissue. However, the relevant literature found that there is no significant change in the total AMPK level in the myocardium. In this work, the p-AMPK level in the H₂O₂ group was lower than that in the control group, and the results may be related to the expression of upstream signals regulating AMPK in ischemic hypoxia-treated cardiomyocytes, such as LKB1 and CaMKK proteins¹⁵.

Researches have shown that AMPK is an agonist of Sirt1, which activates AMPK, which promotes an increase in NAD⁺ biosynthesis of phosphoribosyl transferase (NAMPT), resulting in an increase in the ratio of NAD⁺/NADH and a decrease in nicotinamide levels, which in turn activates another energy receptor "Sirt1"¹⁶. Sirt1 plays a key role in regulating cellular antioxidant stress and inhibiting apoptotic¹⁷. The results of this study disclosed that the expressions of P21, P27, and P53 in the Lenti-PrxII group were significantly decreased. Chen et al¹⁸ have shown that AMPK indirect activators such as metformin cannot directly activate Sirt1 and increase the

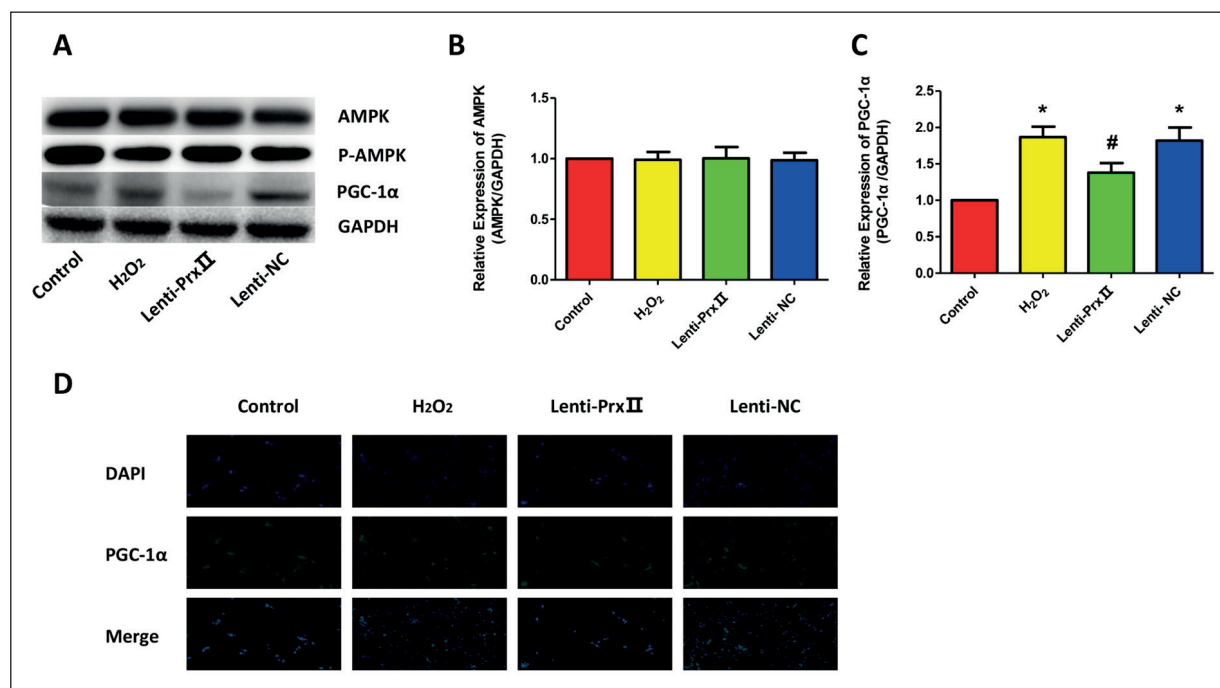


Figure 4. Overexpression of PrxII activates the AMPK pathway. **A**, Western blot is used to detect the expressions of AMPK, p-AMPK, and PGC- α . **B**, AMPK mRNA expression. **C**, PGC- α mRNA expression. **D**, Immunofluorescence is used to detect PGC- α expression (magnification $\times 400$). (“*” indicates statistical difference from the control group $p < 0.05$, “#” indicates statistical difference from the contrast group $p < 0.05$).

ratio of NAD/NADH but play a biological role by promoting the expression of AMPK and then activating the activity of Sirt1.

Sirt1 protein can also be used as an agonist of AMPK protein. Overexpression of Sirt1 promotes lysine deacetylation of LKB1, thereby activating downstream AMPK¹⁹. It can be seen from the experimental results that overexpression of PrxII can promote the expression of Sirt1, but whether it directly targets the target on Sirt1 or promotes the expression of Sirt1 after activating AMPK still needs to be verified by relevant cell experiments.

Conclusions

We demonstrate that overexpression of PrxII activates the AMPK/Sirt1 signaling pathway, thereby inhibiting H₂O₂-induced oxidative stress and slowing apoptosis in H9c2 cells, thus providing a new therapeutic target for ischemic cardiomyopathy.

Conflict of Interest

The Authors declare that they have no conflict of interests.

References

- 1) KANETO CM, NASCIMENTO JS, PRADO M, MENDONCA L. Circulating miRNAs as biomarkers in cardiovascular diseases. *Eur Rev Med Pharmacol Sci* 2019; 23: 2234-2243.
- 2) CADENAS S. ROS and redox signaling in myocardial ischemia-reperfusion injury and cardioprotection. *Free Radic Biol Med* 2018; 117: 76-89.
- 3) CORTASSA S, O'ROURKE B, AON MA. Redox-optimized ROS balance and the relationship between mitochondrial respiration and ROS. *Biochim Biophys Acta* 2014; 1837: 287-295.
- 4) KIM Y, JANG HH. Role of cytosolic 2-Cys Prx1 and Prx2 in redox signaling. *Antioxidants (Basel)* 2019; 8. pii: E169.
- 5) MOON JC, HAH YS, KIM WY, JUNG BG, JANG HH, LEE JR, KIM SY, LEE YM, JEON MG, KIM CW, CHO MJ, LEE SY. Oxidative stress-dependent structural and functional switching of a human 2-Cys peroxiredoxin isotype II that enhances HeLa cell resistance to H₂O₂-induced cell death. *J Biol Chem* 2005; 280: 28775-28784.
- 6) THIRUPATHI A, DE SOUZA CT. Multi-regulatory network of ROS: the interconnection of ROS, PGC-1 alpha, and AMPK-SIRT1 during exercise. *J Physiol Biochem* 2017; 73: 487-494.
- 7) GOWANS GJ, HAWLEY SA, ROSS FA, HARDIE DG. AMP is a true physiological regulator of AMP-activated protein kinase by both allosteric activation and enhancing net phosphorylation. *Cell Metab* 2013; 18: 556-566.
- 8) QI D, YOUNG LH. AMPK: energy sensor and survival mechanism in the ischemic heart. *Trends Endocrinol Metab* 2015; 26: 422-429.
- 9) GUDJONCIK A, GUENANANCIA C, ZELLER M, COTTIN Y, VERGELY C, ROCHETTE L. Iron, oxidative stress, and redox signaling in the cardiovascular system. *Mol Nutr Food Res* 2014; 58: 1721-1738.
- 10) KANAAN GN, HARPER ME. Cellular redox dysfunction in the development of cardiovascular diseases. *Biochim Biophys Acta Gen Subj* 2017; 1861: 2822-2829.
- 11) TSIKAS D. Assessment of lipid peroxidation by measuring malondialdehyde (MDA) and relatives in biological samples: analytical and biological challenges. *Anal Biochem* 2017; 524: 13-30.
- 12) SU S, LI Q, LIU Y, XIONG C, LI J, ZHANG R, NIU Y, ZHAO L, WANG Y, GUO H. Sesamin ameliorates doxorubicin-induced cardiotoxicity: involvement of Sirt1 and Mn-SOD pathway. *Toxicol Lett* 2014; 224: 257-263.
- 13) ZHAO C, ZHANG Y, LIU H, LI P, ZHANG H, CHENG G. Fortunellin protects against high fructose-induced diabetic heart injury in mice by suppressing inflammation and oxidative stress via AMPK/Nrf-2 pathway regulation. *Biochem Biophys Res Commun* 2017; 490: 552-559.
- 14) AL-DAMRY NT, ATTIA HA, AL-RASHEED NM, AL-RASHEED NM, MOHAMAD RA, AL-AMIN MA, DIZMIRI N, ATTEYA M. Sitagliptin attenuates myocardial apoptosis via activating LKB-1/AMPK/Akt pathway and suppressing the activity of GSK-3β and p38α/MAPK in a rat model of diabetic cardiomyopathy. *Biomed Pharmacother* 2018; 107: 347-358.
- 15) SHACKELFORD DB, SHAW RJ. The LKB1-AMPK pathway: metabolism and growth control in tumour suppression. *Nat Rev Cancer* 2009; 9: 563-575.
- 16) VELAGAPUDI R, EL-BAKOUSH A, LEPIARZ I, OGUNRINADE F, OLAJIDE OA. AMPK and SIRT1 activation contribute to inhibition of neuroinflammation by thymoquinone in BV2 microglia. *Mol Cell Biochem* 2017; 435: 149-162.
- 17) KAUPPINEN A, SUURONEN T, OJALA J, KAARNIRANTA K, SALMINEN A. Antagonistic crosstalk between NF-kappaB and SIRT1 in the regulation of inflammation and metabolic disorders. *Cell Signal* 2013; 25: 1939-1948.
- 18) CHEN H, LIU X, CHEN H, CAO J, ZHANG L, HU X, WANG J. Role of SIRT1 and AMPK in mesenchymal stem cells differentiation. *Ageing Res Rev* 2014; 13: 55-64.
- 19) LEE BB, KIM Y, KIM D, CHO EY, HAN J, KIM HK, SHIM YM, KIM DH. Metformin and tenovin-6 synergistically induces apoptosis through LKB1-independent SIRT1 down-regulation in non-small cell lung cancer cells. *J Cell Mol Med* 2019; 23: 2872-2889.